Chain Dynamics in Linear and Hyperbranched Phenol−Polycarbonates

Daniel H. Bolton,[†,§] Jon M. Goetz,[†,⊥] Daoji Gan,[†] Jeffrey A. Byers,[†] Barbara Poliks,[‡] Karen L. Wooley,[†] and Jacob Schaefer*[,†]

Department of Chemistry, Washington University, St. Louis, Missouri 63130, and Department of Physics, Binghamton University, Binghamton, NewYork 13902

Received November 4, 2002

ABSTRACT: Analysis of the macroscopic thermal and mechanical behavior, and microscopic chain packing and dynamics, of two hyperbranched polycarbonates and their compositionally exact linear analogues leads to the conclusion that nearest-neighbor chains (or chain segments) pack and move similarly in linear and hyperbranched systems. However, the distance scale for cooperative motion is much smaller in the hyperbranched polycarbonates, and this leads to mechanical embrittlement.

Introduction

Poly(bisphenol A)carbonate, or polycarbonate, is used extensively as an engineering thermoplastic because of its desirable combination of thermal and mechanical properties.[1,2] Aircraft and automobile parts, optical disk substrates, appliances, and safety glass are just some of the current applications.[3] The introduction of a multifunctional comonomer has been used to incorporate low levels of branching (1−2%) within the polycarbonate structure.[4,5] The resulting material is suitable for blow-molding fabrication of hollow items and large panels.[6] Hyperbranched polycarbonates (more than 50% branching with no cross-links) have been prepared by the polymerization of an A_2B monomer derived from 1,1,1-tris(4′-hydroxyphenyl)ethane.[7] These structures are highly functionalized, globular macromolecules with high solubility, low melt viscosity, and possible applications as low-cost alternatives to dendrimers in composites and coatings.[8,9]

In this paper, we make comparisons between the macroscopic thermal and mechanical behavior of two hyperbranched polycarbonates and their microscopic local chain dynamics. The macroscopic properties are measured by differential scanning calorimetry (DSC), tensile testing, and dynamic mechanical analysis (DMA). The microscopic dynamics are measured by magic-angle spinning ^{13}C NMR. The observed comparisons are interpreted by reference to the properties of linear polycarbonates having repeat units of identical composition to those of the corresponding hyperbranched polycarbonates. Thus, the effects of branching on properties are determined for the same total number of functional side chains and chain ends for both linear and hyperbranched systems (assuming equal molecular weights). The linear polycarbonates are systems for which there are already extensive correlations between macroscopic mechanical behavior, microscopic chain packing, and local chain dynamics.[10−14] In the hyperbranched polycarbonates, cooperative motion can only occur for chain segments that are not directly linked to a branch point. Because the average number of repeat units between branch points is known, the distance scale over which cooperativity can occur is established.

Experimental Section

Materials. Phenol- and *tert*-butyldimethylsilyl ether-terminated linear and hyperbranched polycarbonates (M_W 77 000 and 82 000, respectively) were prepared and characterized as described before.[7] These materials were used for thermal, DMA, and NMR measurements. The degree of branching of the hyperbranched materials was 53%, as determined by HPLC of the degradation products on reduction with lithium aluminum hydride. A few tensile tests were performed on materials prepared in separate batches. The linear phenol−polycarbonate used for tensile testing had M_W of 93 000, while the hyperbranched phenol−polycarbonate had M_W of 10 500. The 2,2′,6,6′-tetrachloropolycarbonate was generously supplied by Dr. E. A. Williams (General Electric Co., Schnectady, NY).

Thermal and Dynamic Mechanical Analysis. Thermal analysis was conducted on a Perkin-Elmer DSC-4 differential scanning calorimeter and on a Perkin-Elmer TGS-2 thermogravimetric analyzer, each upgraded by a temperature-program interface and software package from Instrument Specialist, Inc. (Antioch, IL). DMA was performed on a Rheometrix RSA II dynamic mechanical tester equipped with a low-temperature accessory using liquid nitrogen as a cooling medium. Samples for DMA that were 0.35 cm thick were prepared by heat-pressing polymer powders at 2 metric tons between polyimide sheets at 240 °C for the phenol-containing polymers and 210 °C for the *tert*-butyldimethylsilyl ether-containing polymers. The pressed films were examined at 5 °C increments up to T_g with 0.1% applied strain at 1, 2, 4, 8, and 16 Hz. The frequency dependence of the temperature of the γ-transition loss maximum was used to estimate an apparent Arrhenius activation energy.

Tensile Testing. Strength and modulus properties of linear and hyperbranched phenol−polycarbonates were measured on thin-film specimens (ca. 1 mm thick) at room temperature, according to ASTM D-638. The specimens were prepared by solvent casting from tetrahydrofuran and then cutting into paddle shapes having overall dimensions of 100 mm × 20 mm and a central neck of 40 mm × 10 mm. Two points were drawn onto the samples, within the neck region, at a separation distance of 10 mm, to allow for strain measurements. The Instron was operated in tensile mode (constant strain). The cross-head speed used was 0.1 mm/min. Ten specimens were tested, and five sets of results were used to calculate average values. Tensile strength and elongation were those at the break point. Values of the tensile modulus were determined from the initial slopes of the stress−strain curves.

[†] Washington University.
[‡] Binghamton University.
[§] Present address: Bayer Plastics Division, Pittsburgh, PA 15205.
[⊥] Present address: Varian Associates, Palo Alto, CA 94304.
* Corresponding author: phone 314-935-6844; Fax 314-935-4481; e-mail schaefer@wuchem.wustl.edu.

10.1021/ma021648u CCC: $25.00
Published on Web 03/07/2003

Table 1. Thermal, Mechanical, and NMR Properties of Some Linear and Hyperbranched Polycarbonates

polymer	T_g [°C][a]	T_γ [°C][b]	$E_a(\gamma)$ [kcal/mol]	n_2/n_1 dipolar sideband ratio[c]	fraction mobile sites (f)[d]
tetrachloropolycarbonate	230			1.35	0
linear phenol−polycarbonate	210	−78	11	1.09	0.29
hyperbranched phenol−polycarbonate[e]	205	−92	25	1.06	0.32
silylated linear phenol−polycarbonate	186	−107	21	0.56	0.91
polycarbonate	150	−99	11	0.45	1

[a] From DSC with a heating rate of 20 °C/min. [b] From DMA at 2 Hz. [c] From DRSE ^{13}C NMR with magic-angle spinning at 1859 Hz. [d] From $(n_2/n_1)_{observed} = 0.45f + 1.35(1 - f)$. Estimated accuracy (based on spectral signal-to-nose ratios) is ±10%. [e] T_g of the silylated hyperbranched polycarbonate was 180 °C, and the DRSE n_2/n_1 was 0.53 ($f = 0.88$). This material did not form films suitable for DMA.

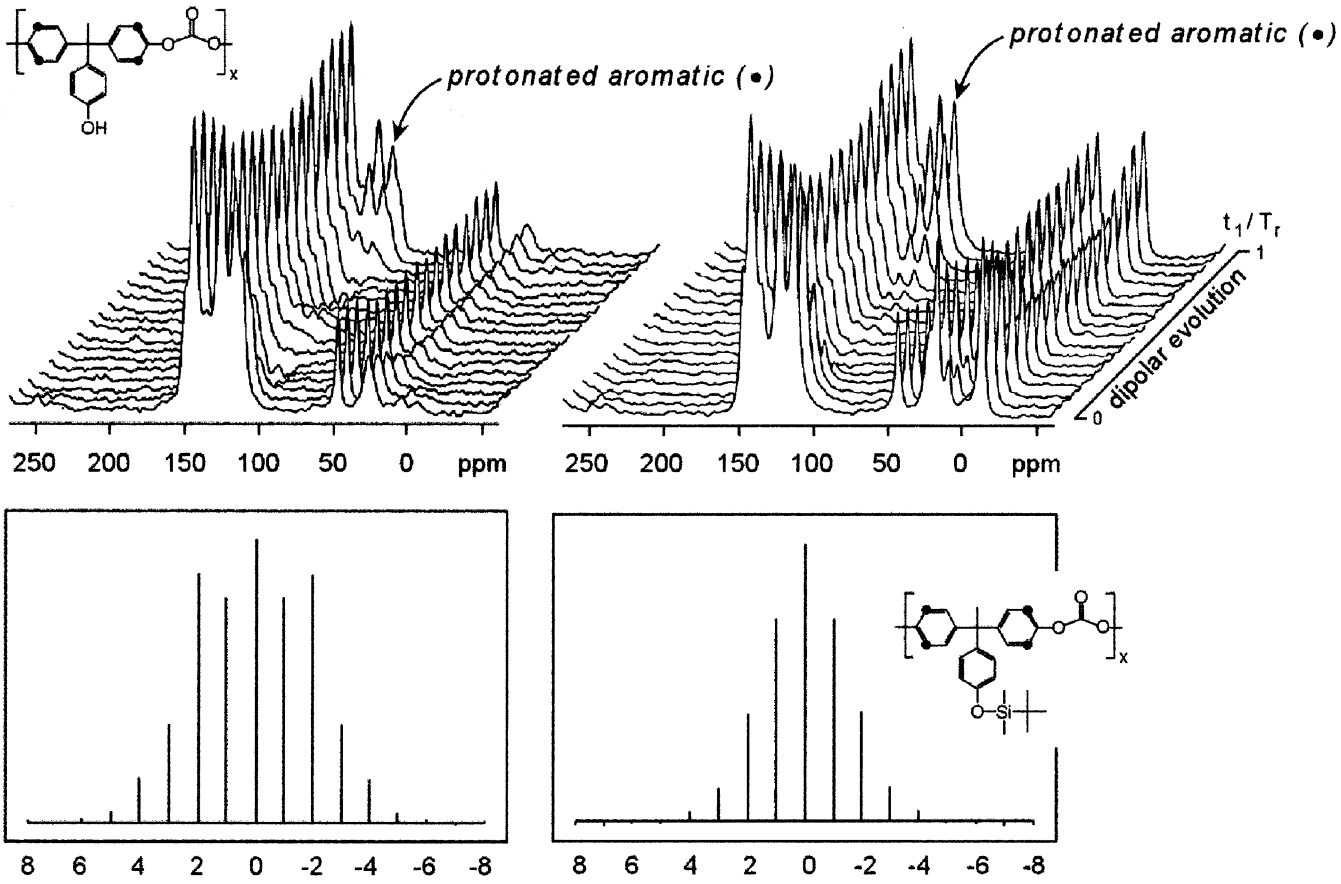

Figure 1. Dipolar rotational spin-echo 15.1 MHz ^{13}C NMR spectra of linear phenol−polycarbonate (left) and silylated linear phenol−polycarbonate (right). The chemical shift spectra in the stack are each incremented by 1/16 of a rotor cycle. The stick spectrum below each stack plot shows the Fourier transform of the dipolar slice at 120 ppm. This shift corresponds to protonated aromatic carbons adjacent to carbonate groups (solid circles). The more gentle modulation of the 120 ppm peak intensity of silylated polycarbonate (no negative-going peaks) means more motion, weaker ^{1}H−^{13}C dipolar coupling, a narrower dipolar pattern, and a reduced n_2/n_1 dipolar sideband ratio. The oxygenated nonprotonated aromatic carbon of phenol side chains appears at 115 ppm. The tail of this line extends to 120 ppm, and this accounts for a slight increase in intensity of the $n = 0$ dipolar sideband peak (lower left panel).

NMR. ^{13}C NMR spectra were obtained at room temperature at 15.1 MHz using a Varian 12 in. resistive magnet (serial no. 55). The single, 11 mm diameter, radio-frequency coil was connected by a low-loss transmission line to a double-resonance tuning circuit. A 1 kW ENI LPI-10H amplifier was used for the ^{1}H channel and an ENI A-300 amplifier for the ^{13}C channel. Cross-polarization transfers were performed at 50 kHz, carbon π pulses were 10 μs, and proton dipolar decoupling was at 100 kHz. Rotors with 600 mg sample capacities were made from plastic (Kel-F) and supported at both ends by air-pumped journal bearings. In these experiments, a 350 mg powder sample was positioned in the center of the rotor by Kel-F spacers.

DRSE. Carbon dipolar line shapes were characterized by dipolar rotational spin-echo (DRSE) ^{13}C NMR with dipolar evolution over one rotor cycle.[15] This is a two-dimensional experiment in which, during the additional time dimension, carbon magnetization is allowed to evolve under the influence of ^{1}H−^{13}C coupling, while ^{1}H−^{1}H coupling is suppressed by homonuclear multiple-pulse semiwindowless MREV-8 decoupling.[16] DRSE is well-suited to the examination of dipolar couplings in unlabeled materials. The cycle time for the homonuclear decoupling pulse sequence was 33.6 μs, resulting in decoupling of proton−proton interactions as large as 60 kHz. Sixteen MREV-8 cycles fit exactly into one rotor period with magic-angle spinning at 1859 Hz. A 16-point Fourier transform of the time dependence of the intensity of any peak resolved by magic-angle spinning yields a 16-point dipolar frequency spectrum, scaled by the MREV-8 decoupling and broken up into sidebands by the spinning. For 15.1 MHz ^{13}C NMR, low-speed spinning produces many DRSE dipolar sidebands with no interferences from chemical shift spinning sidebands.

Broad dipolar powder spectra (Pake patterns) appear for carbons with strong ^{1}H−^{13}C coupling, with narrower patterns observed for carbons with weaker couplings. Because the second spinning sideband is near the maximum of a rigid-

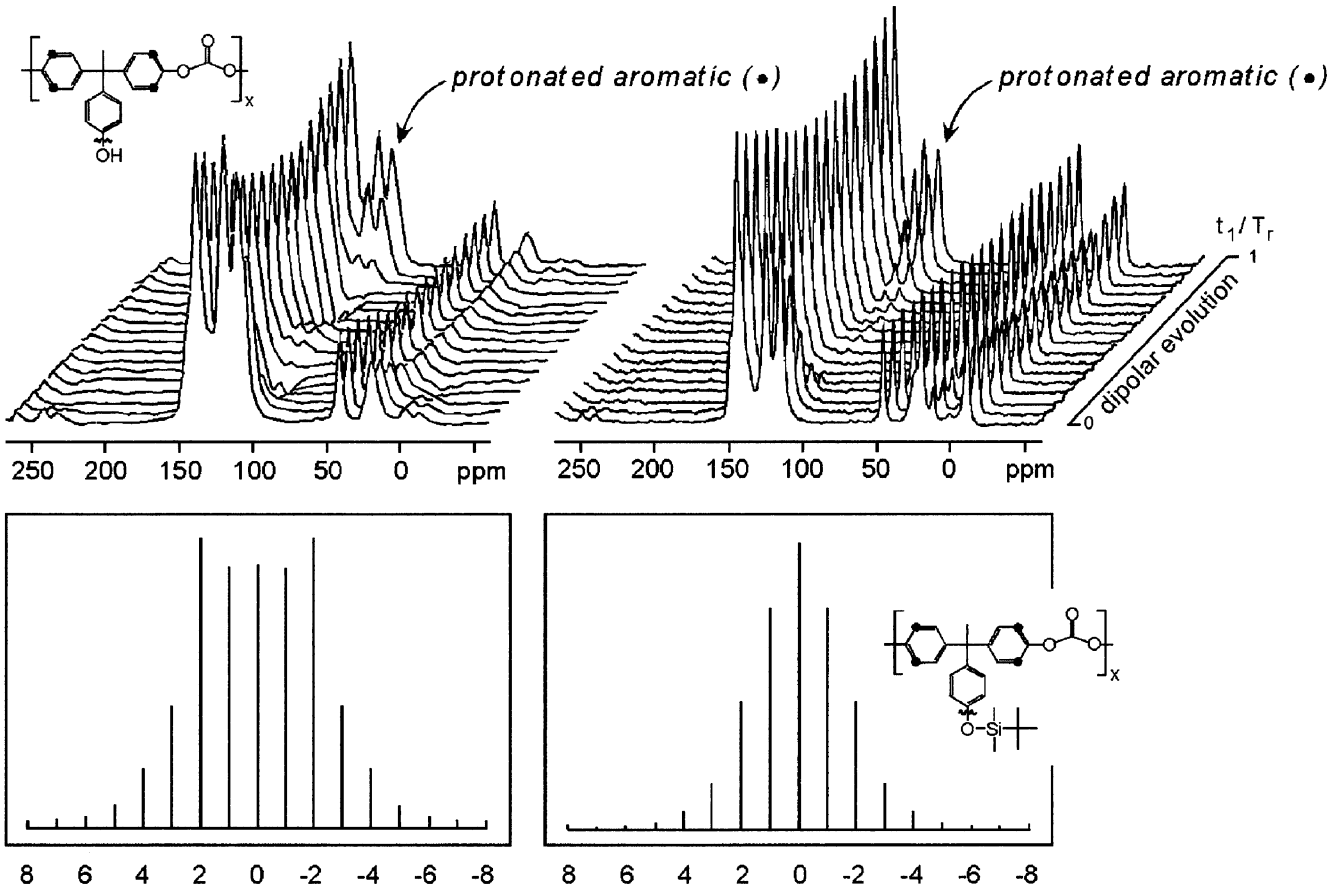

Figure 2. Dipolar rotational spin-echo 15.1 MHz ^{13}C NMR spectra of hyperbranched phenol−polycarbonate (left) and silylated hyperbranched phenol−polycarbonate (right). The stick spectrum below each stack plot shows the dipolar slice at 120 ppm. The chemical shift spectra in the stack are each incremented by 1/16 of a rotor cycle.

lattice dipolar Pake powder pattern under the conditions of our experiments,[17] the ratio of intensities of the second to first dipolar sidebands (n_2/n_1) is a sensitive measure of averaging of the phenylene-ring $^1H-^{13}C$ one-bond dipolar coupling by molecular motion at rates greater than about 10 kHz at 300 K. This ratio changes from about 1.35 in the absence of motion to 0.45 in the presence of 180° ring flips. For a polycarbonate in which ring flips faster than 10 kHz occur only at a fraction, f, of all sites in the glass, $(n_2/n_1)_{obsrvd} = 0.45f + 1.35(1 - f)$, where the observed sideband ratio is that for the 120 ppm protonated, aromatic carbon peak.

The DRSE experiment was calibrated by matching the calculated C−H dipolar sideband spectrum (with a room temperature scale factor[15] of 0.39) for polycrystalline 1,4-dimethoxybenzene.

Molecular Modeling. A hyperbranched structure of phenol−polycarbonate containing 192 units was built and energy-minimized using Cerius2 software (Accelrys Inc., San Diego, CA) with a PCFF force field. The number of repeat units was the same as for the linear phenol−polycarbonate model described in ref 14. Each of the two stereoisomers of the phenol−polycarbonate repeat unit was added randomly to the hyperbranched structure. Monomers were added to the structure with a tendency for a phenol end or side group of one segment to be near the carbonate of another (within 3−5.5 Å). The structure was energy minimized following the addition of every few units. The final structure of 192 units had relative concentrations of branched, linear, and chain-end segments of 26%, 48%, and 26%, respectively, compared to the experimental values[7] of 30%, 47%, and 23%. The structure underwent 15 cycles of simulated annealing for a total of 6 ps. The temperature was changed in 50 °C increments with the starting and mid-cycle temperatures of the annealing at 300 and 500 K, respectively. Each increment contained 50 1 fs steps of molecular dynamics. The structure was energy-minimized after each cycle, and the structure with the lowest energy minimum was used for the illustrations. The density of the final hyperbranched phenol−polycarbonate (single molecule with extended ends) was 0.85 g/cm^3, indicating a bulk density of over 1 g/cm^3.

Results and Discussion

Polycarbonate and Linear Phenol−Polycarbonate. Linear phenol−polycarbonate has a T_g that is 60 °C higher than that of polycarbonate[13] and a well-defined γ-loss transition that is about 20 °C higher (Table 1). In addition, the activation energies of the γ transitions for polycarbonate and phenol−polycarbonate are equal. These results suggest that, qualitatively, local chain dynamics are similar for the two polymers, just shifted in temperature and frequency, consistent with a general stiffening of the phenol−polycarbonate main chain. Recent rotational-echo double-resonance (REDOR) studies of chain packing in linear phenol−polycarbonate[14] have shown that 70% of the repeat units are locally ordered, with a tendency for the phenol moiety of one chain to be proximate to the carbonate group of the nearest-neighbor chain. Thus, the stiffening is likely the result of a combination of interchain hydrogen bonding and increased side chain bulk. Nevertheless, cooperative main chain motions still occur in phenol−polycarbonate. About one-third of the main-chain aromatic rings are undergoing 180° flips at a rate faster than 10 kHz at 300 K ($n_2/n_1 = 1.09$; Table 1 and Figure 1, left).

Molecular dynamics simulations have shown that the gate for aromatic ring flips is the lattice dilation that is

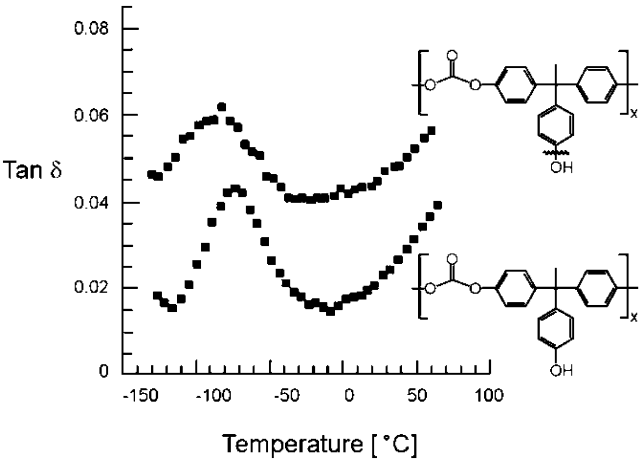

Figure 3. Low-temperature mechanical-loss spectra (at 2 Hz) of linear (bottom) and hyperbranched (top) phenol−polycarbonate. The top spectrum has been translated upward by 0.03 units for clarity.

associated with the γ transition.[18] Main chain aromatic rings wiggle in place until a lattice phonon arrives coincident with the dilation. The jolt of thermal energy pushes the ring over the top of a barrier reduced by the increased separation between chains. The relevant spatial coordinate for this mechanically active two-site flip is not the ring C_2 axis, but a generalized coordinate that depends on the positions of the main chains participating in the lattice dilation.

The two-thirds of the main chain aromatic rings of phenol−polycarbonate that are not flipping faster than 10 kHz at 300 K are probably also flipping, but at slower rates, consistent with the higher temperature γ transition. This sort of modest stiffening of the polycarbonate main chain by addition of bulk to the side chain has been observed before.[10] The added bulk can be accommodated by positioning of the side chain in the open space near the carbonate moiety of the nearest-neighbor chain.[14] By way of contrast, any sort of addition to the main chain aromatic rings has a dramatic effect on chain dynamics. For example, tetrachloropolycarbonate has no observable low-temperature γ transition, and DRSE indicates that none of the rings are mobile (n_2/n_1=1.35, Table 1). Even addition of a methyl group[19] or a single fluorine[20] to a main chain ring is enough to suppress the low-temperature loss peak and block the rings from flipping.

Linear and Hyperbranched Phenol−Polycarbonates. These two polymers have remarkably similar T_g's (Table 1), dipolar sideband ratios (Table 1; Figures 1 and 2), and low-temperature mechanical-loss spectra (Figure 3). The shift to lower temperature and decrease in intensity of the γ transition for the hyperbranched polycarbonate suggest a reduction in size of the cooperative unit participating in the lattice dilation.[18] The average number of repeat units between branch points is only about 3. (The relative concentrations of branched, linear, and chain-end segments are 30%, 47%, and 23%, respectively.[7]) Thus, the motional unit probably only involves two chain fragments, each just 1−2 units in length. For such short chain segments, the lattice dilations leading to ring flips appear to be qualitatively similar in the hyperbranched structure and within full chains in linear phenol−polycarbonate (Figure 1; Table 1, column 5). This is true even though the overall global folding for the two polymers is significantly different.[14]

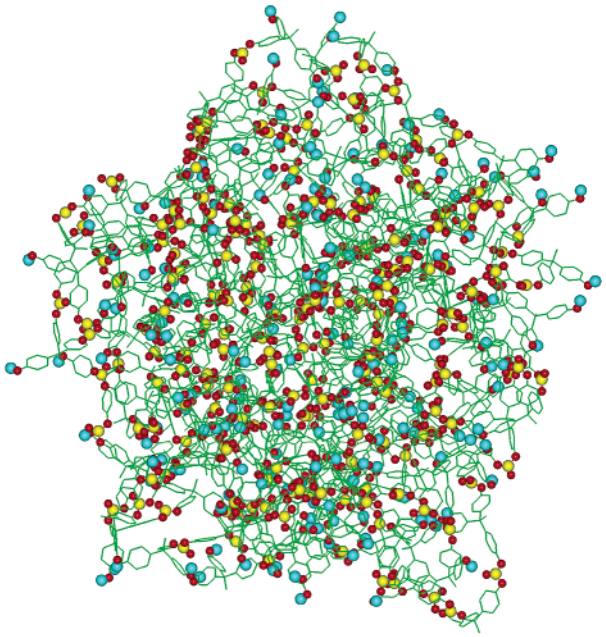

Figure 4. Model of the packing within a single molecule of hyperbranched phenol−polycarbonate. Oxygens are shown in red, the phenol protons in blue, the aromatic rings in green, and the carbonate carbonyl carbon in yellow.

A model for a single hyperbranched phenol−polycarbonate molecule is shown in Figure 4, and an expanded view of the packing within the interior of the strucure is shown in stereo in Figures 5 and 6. The best-fit tendency is for a phenol side chain or end group of one segment to be near the carbonate of another.[14] When nonequilibrium packing is dominated by repulsive enthalpic interactions, then nearest neighbors in the glass will be determined by an entropically driven (largest selection) of best fits (minimum repulsions).[21,22] Nearest-neighbor pairs of segments in this situation are apparently capable of forming a molecular gate because about one-third of the rings in hyperbranched polycarbonate are flipping faster than 10 kHz at 300 K (n_2/n_1 = 1.06, Table 1). In hyperbranched polycarbonate, the ends of motionally cooperative units are necessarily near inflexible covalent branch points. This makes a lattice dilation difficult, which results in an activation energy for the γ transition of 25 kcal/mol, more than double the value for linear phenol−polycarbonate (Table 1).

The restricted scale of cooperative motion in hyperbranched polycarbonate means that the material is brittle. Ductility (plastic deformation) requires cooperative main chain motion on a large scale, including perhaps as many as 5−7 repeat units along a single polycarbonate chain.[23] Such motion lowers the yield stress below the critical value at which brittle failure of the material will occur.[24] Large-scale cooperative motion may also collapse nanovoids (the gaps between chains) so that craze initiation sites are avoided.[25] Without large-scale cooperative motion, a brittle fracture is inevitable. Nevertheless, hyperbranched phenol−polycarbonate is the first example of a hyperbranched polymer that can be formed into films of suitable integrity to withstand traditional mechanical analysis as bulk samples. Instron analysis (ASTM method D-638) performed on a hyperbranched phenol−polycarbonate (10 500 M_w) gave a tensile strength (ultimate) of 3.9 ± 0.3 MPa, elongation to rupture of 9.2 ± 1.4%, and tensile modulus of 1050 ± 35 MPa. The relatively low values

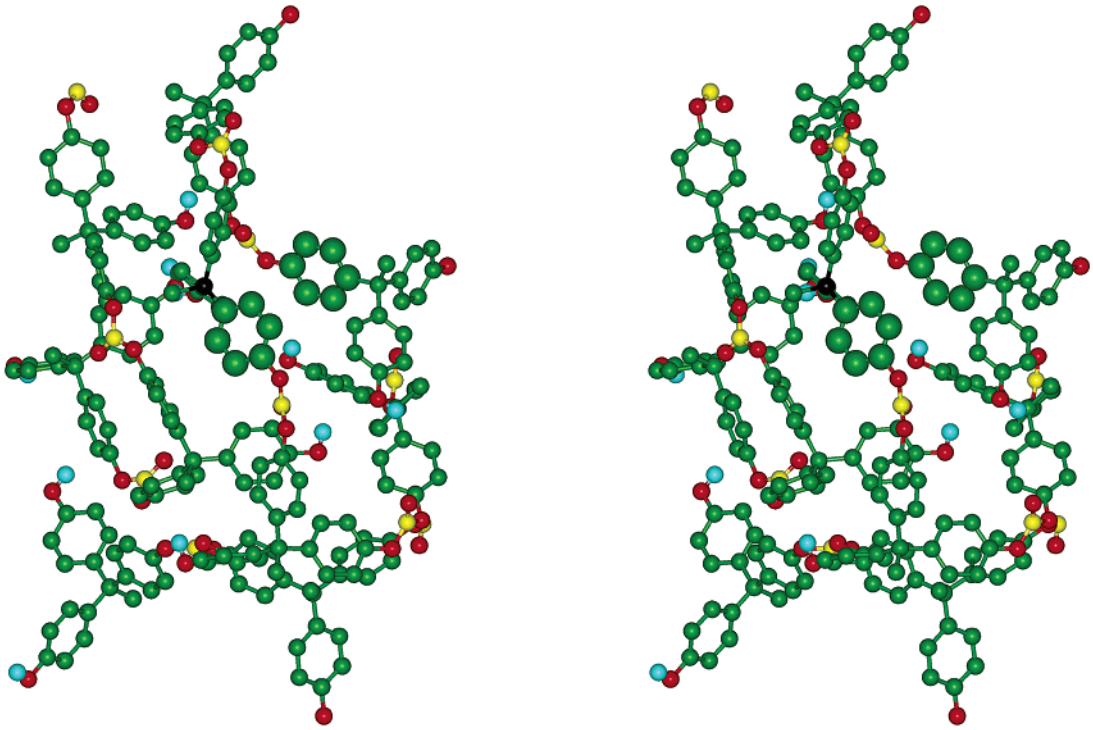

Figure 5. A few repeat units of the structure of Figure 4 shown in stereo. The tendency for the phenol chain ends and side chains to be near a carbonate mimics the packing behavior of phenol side chains and carbonate groups in linear phenol–polycarbonate (see Figure 8 of ref 14). The aromatic ring attached to the quaternary carbon in black has a nearest-neighbor ring (just to the right and slightly above), which is in position to act as a ring-flip gate. These two rings are highlighted by size.

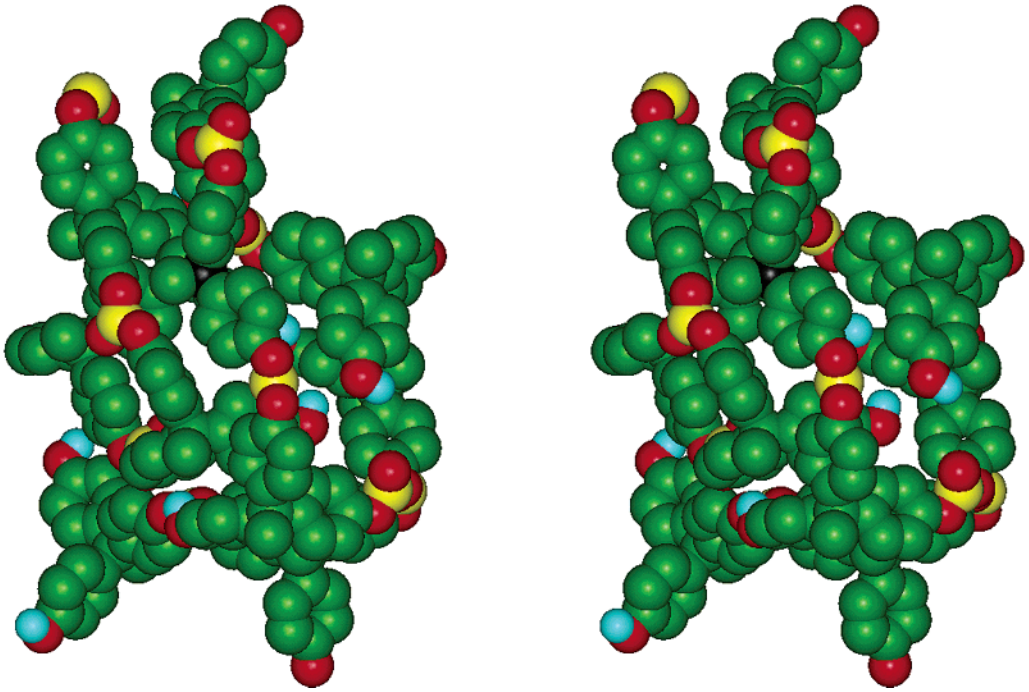

Figure 6. Space-filling version (without a size highlight) of the repeat units of Figure 5.

for these measurements are consistent with a lack of chain entanglements, which is due to both low molecular weight and the presence of branching. For a linear phenol–polycarbonate (93 000 M_w), the Instron analysis gave a tensile strength (ultimate) of 80 ± 9 MPa, elongation to rupture of 75 ± 6%, and tensile modulus of 2520 ± 120 MPa.

Silylation of Linear and Hyperbranched Phenol–Polycarbonates. Silylation eliminates the possibility of hydrogen bonding, and this decreases the T_g of linear phenol–polycarbonate by 24 °C (Table 1). There is a similar decrease of 25 °C for hyperbranched phenol–polycarbonate on silylation. The silylation introduces a 5-methyl group cluster that apparently acts as a steric wedge to separate nearest-neighbor chains enough to enable a ring flip. We reach this conclusion for both linear and hyperbranched systems because silylation makes virtually all main chain rings mobile on a 10 kHz frequency scale ($n_2/n_1 \approx 0.5$, Figures 1 and 2). For silylated linear phenol–polycarbonate relative to linear

phenol−polycarbonate itself, the cooperative motional unit gating the fast ring flips is reduced in size (T_γ is lowered by 8 °C) and isolated in space (E_a is increased by 10 kcal/mol). The high concentration of silyl wedges restricts cooperativity to just a few chains. The result of this mechanical insulation is embrittlement, which was apparent in the observed fragility of the DMA sample strips. In fact, the corresponding silylated hyperbranched phenol−polycarbonate was so brittle it was impossible to make films suitable for DMA. The brittleness of the silylated hyperbranched polycarbonate underscores the fact that those lattice dilations which are monitored by ring flips are a necessary but not sufficient condition for ductility.[26]

The existence of fast ring flips at almost all sites in silylated hyperbranched phenol−polycarbonate (with its extensive network of both covalent and steric insulators) means that the gate need be no more than the cooperative motion of a pair of rings on adjacent chains. This was the surmise that formed the basis of the Whitney−Yaris description[18] of the ring-flip process in polycarbonate using generalized Langevin dynamics.

Acknowledgment. This work was supported by ARO Grant DAAG 55-97-1-0183 and ONR Grant N00014-02-1-0326 (K.L.W.) and by NSF Grant DMR-97202 (J.S.).

References and Notes

(1) Clagett, D. C.; Shafer, S. J. *Comprehensive Polymer Science: The Sythesis, Characterization, Reactions, and Applications of Polymers;* Eastmond, G. C., Ledwith, A., Russo, S., Sigwalt, P., Eds.; Pergamon Press: Oxford, 1989; Vol. 5, pp 345−356.
(2) Schnell, H. *Chemistry and Physics of Polycarbonates, Polymer Reviews*, Bd. 9; Interscience: New York, 1964.
(3) Committee on Polymer Science and Engineering, National Research Council. *Polymer Science and Engineering: The Shifting Research Frontiers;* National Academy Press: Washington, DC, 1994; pp 68−70.
(4) Frietag, D.; Haberland, U.; Krimm, H. U.S. Patent No. 3,799,953, 1974.
(5) Mark, V.; Hedges, C. V. U.S. Patent No. 4,469,861, 1984.
(6) Stinson, S. C. *Chem. Eng. News* **1990**, May 7, 55.
(7) Bolton, D. H.; Wooley, K. L. *J. Polym. Sci., Part A: Polym. Chem.* **2002**, *40*, 823.
(8) Hawker, C. J.; Chus, F.; Pomery, P. J.; Hill, D. J. T. *Macromolecules* **1996**, *29*, 3831.
(9) Gaynor, S. G.; Edelman, S.; Matyjaszewski, K. *Macromolecules* **1996**, *29*, 1079.
(10) Schaefer, J.; Stejskal, E. O.; McKay, R. A.; Dixon, W. T. *Macromolecules* **1984**, *17*, 1479.
(11) Schmidt, A.; Kowalewski, T.; Schaefer, J. *Macromolecules* **1993**, *26*, 1729.
(12) Goetz, J. M.; Wu, J.; Yee, A. F.; Schaefer, J. *Macromolecules* **1998**, *31*, 3016.
(13) Klug, C. A.; Zhu, W.; Tasaki, K.; Schaefer, J. *Macromolecules* **1997**, *30*, 1734.
(14) O'Connor, R. D.; Poliks, B.; Bolton, D. H.; Goetz, J. M.; Byers, J. A.; Wooley, K. L.; Schaefer, J. *Macromolecules* **2002**, *35*, 2608.
(15) Schaefer, J.; McKay, R. A.; Stejskal, E. O.; Dixon, W. T. *J. Magn. Reson.* **1983**, *52*, 123.
(16) Rhim, W. K.; Elleman, D. D.; Vaughan, R. W. *J. Chem. Phys.* **1973**, *59*, 3740.
(17) Garbow, J. R.; Schaefer, J. *Macromolecules* **1987**, *20*, 819.
(18) Whitney, D.; Yaris, R. *Macromolecules* **1997**, *30*, 1741.
(19) Klug, C. A.; Wu, J.; Xiao, C.; Yee, A. F.; Schaefer, J. *Macromolecules* **1997**, *30*, 6302.
(20) Wu, J.; Xiao, C.; Yee, A. F.; Goetz, J. M.; Schaefer, J. *Macromolecules* **2000**, *33*, 6949.
(21) O'Connor, R. D.; Byers, J. A.; Aronold, W. D.; Oldfield, E.; Wooley, K. L.; Schaefer, J. *Macromolecules* **2002**, *35*, 2618.
(22) Davidchack, R. L.; Laird, B. B. *J. Chem. Phys.* **1998**, *108*, 9452.
(23) Xiao, C.; Jho, J. Y.; Yee, A. F. *Macromolecules* **1994**, *27*, 2761.
(24) Chen, L.; Yee, A. F.; Goetz, J. M.; Schaefer, J. *Macromolecules* **1998**, *31*, 5371.
(25) Liu, J.; Yee, A. F. *Macromolecules* **2000**, *33*, 1338.
(26) Schaefer, J.; Stejskal, E. O.; Perchak, D.; Skolnick, J.; Yaris, R. *Macromolecules* **1985**, *18*, 368.

MA021648U